Bioorganic & Medicinal Chemistry Letters 25 (2015) 4370–4381

Contents lists available at ScienceDirect

Bioorganic & Medicinal Chemistry Letters

journal homepage: www.elsevier.com/locate/bmcl

Digest paper

Neutrophil elastase inhibitors for the treatment of (cardio) pulmonary diseases: Into clinical testing with pre-adaptive pharmacophores

Franz von Nussbaum [a], Volkhart M.-J. Li [b]

[a] Bayer HealthCare AG, Medicinal Chemistry Berlin, 13353 Berlin, Germany
[b] Bayer HealthCare AG, Lead Discovery Wuppertal, 42096 Wuppertal, Germany

ARTICLE INFO

Article history:
Received 1 June 2015
Revised 14 August 2015
Accepted 20 August 2015
Available online 20 August 2015

Keywords:
Elastase inhibitors
Medicinal chemistry
Biological activity
Protease–antiprotease balance
COPD
Induced fit
PAH
Heterocyclic chemistry

ABSTRACT

Alpha-1 antitrypsin deficiency is linked with an increased risk of suffering from lung emphysema. This discovery from the 1960s led to the development of the protease–antiprotease (im)balance hypothesis: Overshooting protease concentrations, especially high levels of elastase were deemed to have an destructive effect on lung tissue. Consequently, it was postulated that efficient elastase inhibitors could alleviate the situation in patients. However, despite intensive drug discovery efforts, even five decades later, no neutrophil elastase inhibitors are available for a disease-modifying treatment of (cardio)pulmonary diseases such as chronic obstructive pulmonary disease. Here, we critically review the attempts to develop effective human neutrophil elastase inhibitors while strongly focussing on recent developments. On purpose and with perspective distortion we focus on recent developments. One aim of this review is to classify the known HNE inhibitors into several generations, according to their binding modes. In general, there seem to be three major challenges in the development of suitable elastase inhibitors: (1) assuring sufficient potency, (2) securing selectivity, and (3) achieving metabolic stability especially under pathophysiological conditions. Impressive achievements have been made since 2001 with the identification of potent nonreactive, reversible small molecule inhibitors. The most modern inhibitors bind HNE via an induced fit with a frozen bioactive conformation that leads to a significant boost in potency, selectivity, and stability ('pre-adaptive pharmacophores'). These 5th generation inhibitors might succeed in re-establishing the protease–antiprotease balance in patients for the first time.

Human neutrophil elastase (HNE, EC 3.4.21.37) is a proteolytic enzyme belonging to the chymotrypsin-like family of serine proteases. This highly active protease has revealed a broad substrate specificity and is one of the few proteases which are able to degrade the extracellular matrix protein elastin, giving rise to the enzyme's name. In particular, HNE is capable of breaking down mechanically important structures of (1) the body's own cellular matrix (e.g., proteins like collagen and fibronectin) and (2) foreign proteins (e.g., the outer cell wall proteins of Gram-negative bacteria). Furthermore, the enzyme cleaves a variety of endogenous and exogenous proteins thereby modulating their biological activity, including (1) activation of other bioactive proteases, (2) liberation of growth factors and the shedding of cell-surface-bound receptors, and (3) inactivation of endogenous proteinase inhibitors and exogenous virulence factors. In summary, HNE plays a pivotal role in the innate immune response (host defense against bacteria), in tissue remodeling processes, and in the onset and resolution of inflammation.[1]

The activity of this Janus-faced protease is strictly regulated to avoid uncontrolled proteolysis and inflammation in the body by (1) channeling the potentially devastating protease to specialized compartments (e.g., storage in azurophil granula in the cytoplasm of neutrophils), and (2) the presence of extracellular neutralizing, endogenous serine protease inhibitors (SERPINs), for example, alpha-1 antitrypsin (AAT, also known as alpha-1 proteinase inhibitor, α-1 PI), which constitute and maintain the protease–antiprotease balance.[2,3]

Abbreviations: AAT, alpha-1 antitrypsin (alpha-1 proteinase inhibitor, α-1 PI); AATD, alpha-1 antitrypsin deficiency; ALI, acute lung injury; ARDS, acute respiratory distress syndrome; BE, bronchiectasis; CF, cystic fibrosis; COPD, chronic obstructive pulmonary disease; DMPK, drug metabolism and pharmacokinetics; HNE, human neutrophil elastase; NCF, non-cystic fibrosis; NE, neutrophil elastase; NSCLC, non-small cell lung carcinoma; PAH, pulmonary arterial hypertension; PH, pulmonary hypertension; SIRS, systemic inflammatory response syndrome; SMOL, small molecule.

E-mail addresses: franz.nussbaum@bayer.com (F. von Nussbaum), volkhart.li@bayer.com (V.M.-J. Li)

http://dx.doi.org/10.1016/j.bmcl.2015.08.049
0960-894X/

The azurophil granula contain a protecting, acidic milieu prohibiting any proteolytic activity. However, elastase is activated via mild alkalosis during the fusion of the granula with vacuoles that carry bacteria. This step generates so called phagolysosomes, the site where engulfed bacteria are destroyed (Fig. 1, step 1; Table 1).[4,5] Upon neutrophil activation, the intracellular granula fuse with the cell membrane which dramatically enlarges the neutrophil cell surface area (lamellipodia phenotype) and triggers a neutrophil oxidative burst (Fig. 1, step 2). Active enzyme is then liberated into the extracellular space with approximately 10% of the secreted elastase bound to the neutrophil cell membrane. From this point on 'free' elastase can potentially be neutralized by binding of antiproteases that are abundantly found in plasma. However, at the site of liberation, the millimolar concentration of elastase still outcompetes the micromolar concentration of extracellular antiprotease. More distant from the site of degranulation, the elastase concentration decreases due to diffusion/dilution until 'free' elastase is completely neutralized. Consequently, only a small space of obligate elastase activity exists around activated neutrophils in a healthy situation.[6–8]

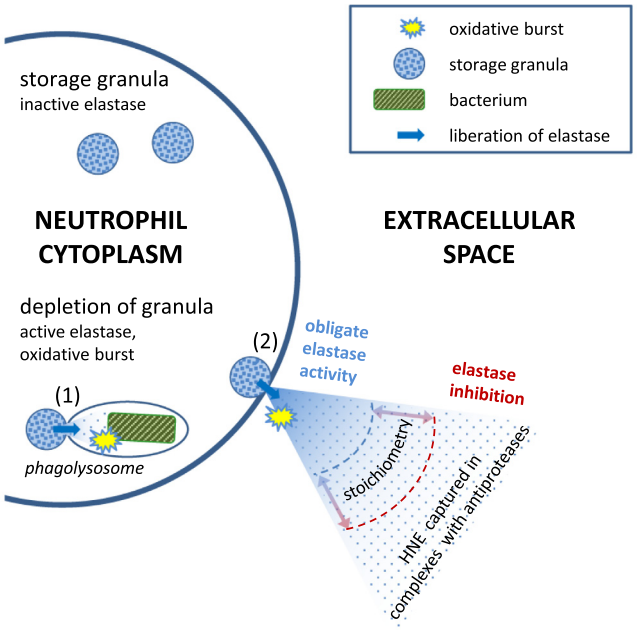

Figure 1. Schematic representation of the human neutrophil elastase (HNE) life cycle: Elastase is activated during the depletion of the acidic storage granula (circles) and (1) liberated into the cytoplasmic phagolysosomes (oval) with engulfed bacteria (green rectangle) or (2) into the extracellular space. Free extracellular elastase is neutralized via binding to antiproteases. The efficiency of neutralization depends on the spatiotemporal stoichiometry of both binding partners, details see Figure 16. Besides HNE, the storage granula bear two further proteases (cathepsin G, proteinase 3) and the enzyme myeloperoxidase (MPO) involved in the neutrophil oxidative burst (yellow star).

Table 1
Relationship of the neutrophil state to elastase localization and biological function (NET = neutrophil extracellular trap)

Neutrophil state	Elastase localization	Biological function
Resting	Intracellular (granula)	Storage
Activated	Intracellular (phagolysosome)	Host defense
Activated	Extracellular (free and membrane-bound)	Inflammatory response, tissue remodeling
Dying	Extracellular (NET-bound)	Resolution of inflammation, host defense

On the other hand, elastase is also involved in the resolution of the inflammation (Table 1). Activated, pro-inflammatory neutrophils enter an elastase-dependent programmed cell death process (NETosis) where elastase is translocated to the cell nucleus and undergoes condensation with DNA and histone proteins. Then the dying neutrophils disintegrate and produce neutrophil extracellular traps (NETs) comprised of long extracellular 'filaments' of DNA with bound proteins, such as histones, elastase, and myeloperoxidase (MPO). These filaments are also able to trap bacteria and fungi, and hamper a fast spread of these microorganisms.[9,10]

Out-of-balance elastase activity contributes to the onset and progression of many inflammatory diseases with severe impact on organ tissue integrity. Chronic obstructive pulmonary disease (COPD) is regarded as the traditional target indication for any elastase inhibitor treatment therapy since a cohort of humans lacking sufficient amounts of the antiprotease AAT demonstrated a significantly higher risk of suffering from lung emphysema as a common form of COPD (AAT-deficiency, AATD as defined above).[11] In addition to the common disease COPD, some other more rare inflammatory conditions or orphan diseases are also characterized by a disturbed protease–antiprotease balance (Fig. 2). There is also good evidence for this out-of-balance elastase activity from experimental pharmacological data with protease knockout or transgenic antiprotease rodents in pulmonary disease models.[12–18] In this review, we focus on (cardio)pulmonary diseases only, such as COPD, cystic fibrosis (CF), bronchiectasis (BE), pulmonary arterial hypertension (PAH), pulmonary fibrosis, and acute lung injury (ALI). Other important neutrophil-driven inflammatory diseases, such as rheumatoid arthritis and inflammatory bowel disease, will not be discussed.

Evolution of relevant (clinical) HNE inhibitors: There is a high medical need for neutrophil elastase inhibitors due to the key role of neutrophil elastase in inflammation as well as (lung) tissue degradation and remodeling. In the last three decades many stakeholders in academia and the pharmaceutical industry have discovered a variety of innovative elastase inhibitors. We will briefly summarize this evolution of HNE inhibitors along five generations. Beginning with biologicals (1st generation), ultimately a novel *pre-adaptive pharmacophore model* has given rise to presumably the best-in-class elastase inhibitors to date (5th generation). Many of these compounds have picomolar potency, are highly selective and show drug-like pharmacokinetics.

Although neutrophil elastase inhibitors from natural products have been described frequently (e.g., flavonoids, cinnamic and caffeic acid derivates, and cyclic peptolides), many of these small to mid-size molecules have revealed only a weak or moderate potency, limited selectivity, and serious metabolic liabilities which

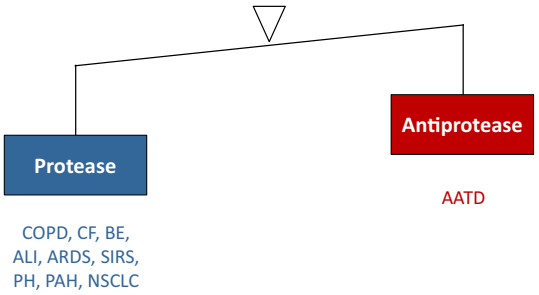

Figure 2. Protease–antiprotease imbalance in pulmonary diseases: Elastase potentially plays a key role in many pulmonary diseases where the protease–antiprotease balance is disturbed.

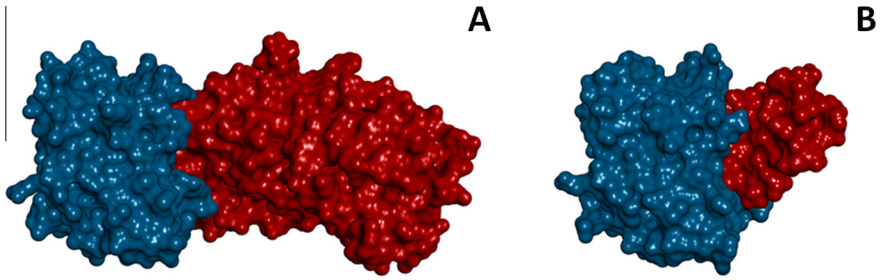

Figure 3. Selection of 1st generation neutrophil elastase inhibitors (biologicals): (A) α-1 PI (Prolastin®, Zemaira®, Aralast®; K_i < 0.1 nM) and (B) elafin (tiprelestat, K_i 0.08 nM) displayed as the protease–antiprotease complexes. The different size of both antiproteases is notable. Both figures were generated by superimposing an in-house neutrophil elastase crystal structure with PDB entries 2D26 and 1FLE, respectively, using the program Discovery Studio. (A) Porcine pancreatic elastase (dark blue)/α-1 PI (bordeaux red); (B) porcine pancreatic elastase (dark blue)/elafin (bordeaux red).

have hampered sound preclinical and clinical testing so far.[19] As such early-stage inhibitors have been reviewed elsewhere,[19] they will not be further considered here.

1st generation (biologicals): Following the principal idea of highly specific, complementary binding partners, as proposed in H.E. Fischer's *Lock and Key Model*, the 1st generation of neutrophil elastase inhibitors commenced with the natural counterparts of elastase. For example, the endogenous antiprotease α-1 PI (Prolastin®, Zemaira®, Aralast®) compromises a highly complementary tertiary structure to elastase and has been used as an augmentation therapy for AATD patients (Fig. 3). Originally isolated from human plasma, modern variants are derived from recombinant sources to better accommodate potential safety and cost issues.[20,21] The most important antiproteases are α-1 PI (AAT), elafin, and secretory leukocyte protease inhibitor (SLPI) which are capable of inhibiting the most prominent neutrophil serine proteases stored in the cytoplasmic azurophil granula: HNE, proteinase 3 (PR3), and cathepsin G (CatG).

The antiproteases interact along the enzyme's substrate binding cleft covering manifold contacts with the target at the substrate pockets S5–S3′ (nomenclature according to Schechter and Berger) which translates into a very tight, pseudo-irreversible binding (Fig. 4).

A major drawback of these 1st generation inhibitors is a lack of stability especially under pathophysiological, oxidative stress conditions: (1) host and/or microbial proteases can partially degrade the antiproteases and thereby impede the inhibitory function,[22,23] and (2) oxidation of vulnerable methionine residues results in a significantly lower inhibitory capacity.[24–27] In addition, α-1 PI is unable to efficiently inhibit membrane-bound neutrophil elastase.[28] This is most probably due to a steric hindrance of this large antiprotease and the unique conformational change upon binding its protease counterpart, translocating the antiprotease on the opposed side of the protease.[29]

Furthermore, the intrinsic physicochemical properties of these biologicals allow only for an intravenous or a potentially inhalative administration route, and thus hamper a broad and repetitive oral usage in chronic diseases like COPD. Consequently, their current clinical development is focused on more acute settings with intravenous or inhaled applications, such as clinical Phase II tests with (1) elafin (tiprelestat) for the prevention and treatment of postoperative inflammatory complications in esophagus carcinoma surgery, coronary artery bypass surgery, and kidney transplantation,[30] or (2) AAT for the prevention of bronchiolitis obliterans syndrome (BOS) in lung transplant recipients,[31] acute graft-versus-host disease,[32,33] acute inflammatory response in acute myocardial infarction,[34] and post-cardiac surgery systemic inflammatory response.[35]

2nd generation (mechanism-based suicide SMOLs): Along the lines of Paul Ehrlich's *Pharmacophore Model*, a more detailed analysis of the substrate recognition and enzymatic reaction mechanism of serine proteases led to the first small molecule (SMOL) inhibitors with active-site recognition. In order to ensure sufficient potency these inhibitors were typically based on a covalent reversible or irreversible binding mechanism.

In contrast to the 1st generation elastase inhibitors, these low-molecular weight molecules are, in principle, able to reach and inhibit also membrane-bound elastase (see Fig. 1). Of further importance, such inhibitors might be able to enter neutrophil cells and thereby interfere with the host defense function of elastase. First examples have been various peptide-based SMOL inhibitors or peptidomimetics, followed by non-peptide-based inhibitors (Fig. 5). In general, all these 2nd generation inhibitors have displayed a mechanism-based, reactive mode of action (suicide

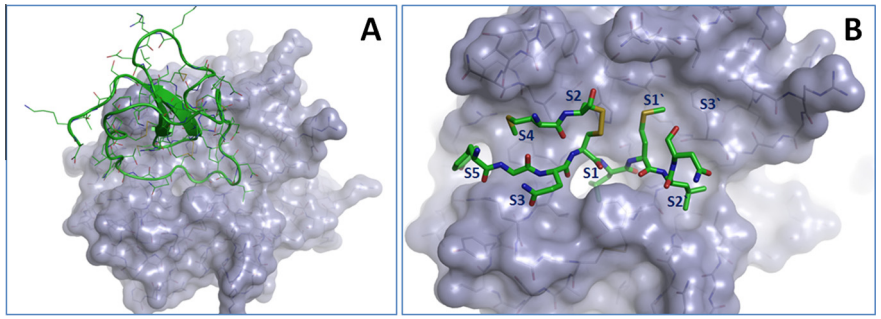

Figure 4. Crystal structure of HNE in complex with 1st generation inhibitor SLPI (green; PDB entry 2Z7F): The protease is shown in a stick representation with transparent Connolly-like surface (grey). (A) View from above into the substrate binding cleft of HNE (grey); the domain of the antiprotease involved in protein–protein interactions with HNE is displayed in helix/ribbon and backbone representation (green) with side-chain residues in sticks; (B) detailed view of the HNE substrate binding cleft with labeled subsites S5–S4–S3–S2–S1–S1′–S2′–S3′ and the bound SLPI inhibitory loop residues in sticks (carbon, green; oxygen, red; nitrogen, blue; sulfur, yellow). The inhibitory loop perfectly fills the substrate binding cleft characterized by the deep S1 pocket.

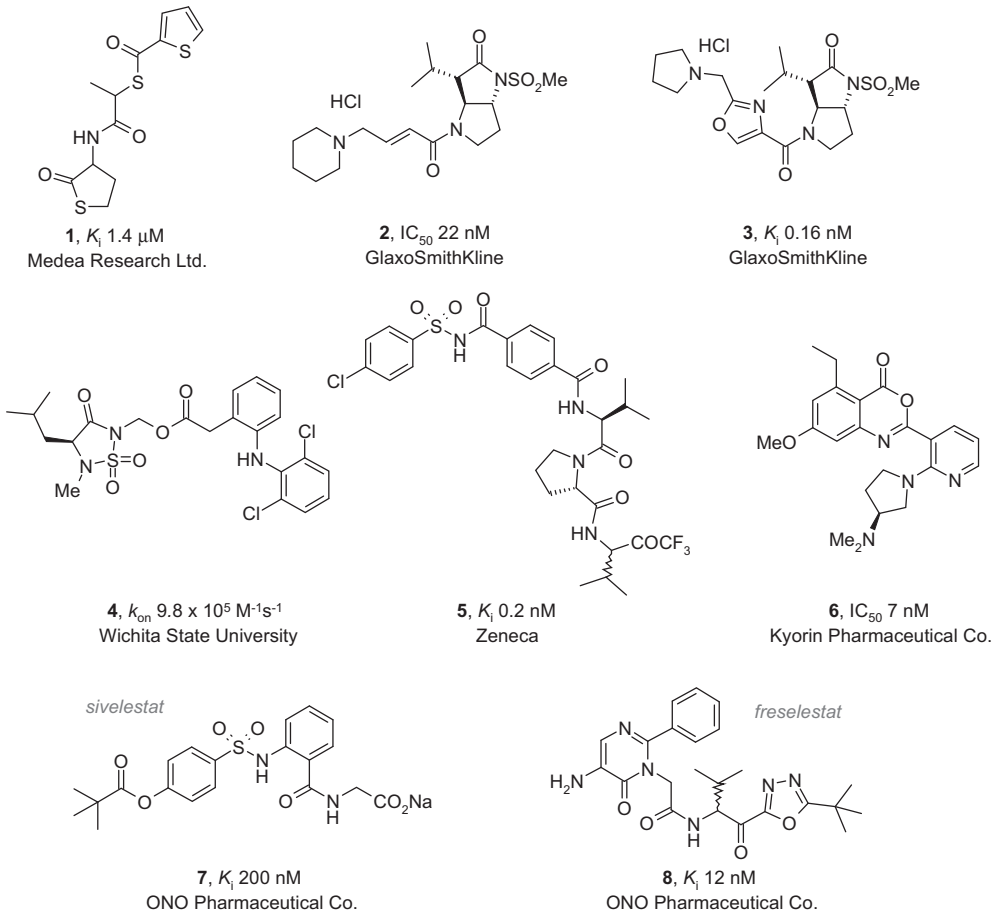

Figure 5. Selection of 2nd generation neutrophil elastase inhibitors (SMOLs, suicide inhibitors): MR-889 (**1**, midesteine), GW311616A (**2**), GW475151 (**3**), 1,2,5-thiadiazolidin-3-one **4**, ICI 200,880 (**5**), AX-9657 (**6**), ONO-5046 (**7**, sivelestat, Elaspol®), and ONO-6818 (**8**, freselestat).

inhibitors) and can be roughly categorized into classes of acylators, Michael acceptors, or electrophilic ketones (transition-state mimics). Almost every large pharmaceutical company has had an elastase inhibitor program, resulting in a myriad of HNE inhibitors with many different reactive pharmacophores.[19,36–41]

These mechanism-based elastase inhibitors interact in a covalent manner with the enzyme's active site, namely by electrophilic attack of Ser^{195} (chymotrypsin numbering, Fig. 6). A proper positioning of the reactive moiety of the inhibitor is achieved through guiding interactions of the P4–P1, P2′, and P3′ residues of the inhibitor (Fig. 7). Thus, similar to the 1st generation elastase inhibitors, the interaction with the target basically occurs along the substrate binding cleft (Fig. 8).[42] In general, interaction with the P1 moiety of a substrate or inhibitor is reflected as the most assertive interaction with regard to target specificity, matching the pronounced S1 binding pocket.[43,44]

However, due to the inherent reactive nature of these inhibitors, the compounds in general suffer from not optimal pharmacokinetic properties (metabolic liabilities) and/or adverse events (due to lack of specificity). Not surprisingly, few compounds have revealed acceptable drug-like properties allowing for a safety and efficacy assessment in humans. Overall, the clinical outcome has been disappointing with only sivelestat (**7**, Elaspol®) reaching the market for the treatment of ALI/ARDS in Japan and South Korea in 2002 and 2006. To date, efforts to enlarge the country or indication scope of Elaspol® have failed.

Sivelestat (**7**) has only a moderate potency (K_i 200 nm) and selectivity versus off-targets such as porcine pancreatic elastase (IC_{50} 5.6 μm).[45] The drug has to be administered strictly intravenously, as the pharmacokinetic profile does not allow for an oral administration.[46,47] The clinical efficacy of sivelestat (**7**) remains controversial. Local Japanese studies and multinational studies on the treatment of patients with ALI associated with SIRS have revealed seemingly inconsistent results with regard to improvements in ventilator-free days, ICU-free days, and long-term survival.[48–52]

3rd and 4th generation (modern, non-mechanism-based SMOLs): The 3rd and 4th generation of neutrophil elastase inhibitors are characterized by nonreactive, reversible inhibitors originating from pyridone and dihydropyrimidinone lead structures independently published by AstraZeneca in 2002 and Bayer in 2001 (Figs. 9 and 10). A unique binding mode in the active center of the enzyme (S1 pocket) triggers a conformational change in the protease creating a *de novo* formed deep S2 pocket enabling further unprecedented target interactions.[53] This remarkable binding feature could be described as being analogous to the *Induced Fit Model* proposed by D.E. Koshland. Notably, this interaction does not follow the linear topology of the substrate binding cleft as it is the case with the 1st and 2nd generation inhibitors. On the contrary, the orientation of 3rd and 4th generation inhibitors is almost perpendicular to the natural substrate binding cleft. Whereas 3rd generation inhibitors only occupy the S1 pocket of the enzyme, 4th generation inhibitors also bind to the deepened S2 pocket.

Based on their improved drug-like properties the two new lead structure series were highly stimulating for the preclinical development of elastase inhibitors and elicited a lot of activity both within companies and beyond.[19,54–57] To date, two optimized,

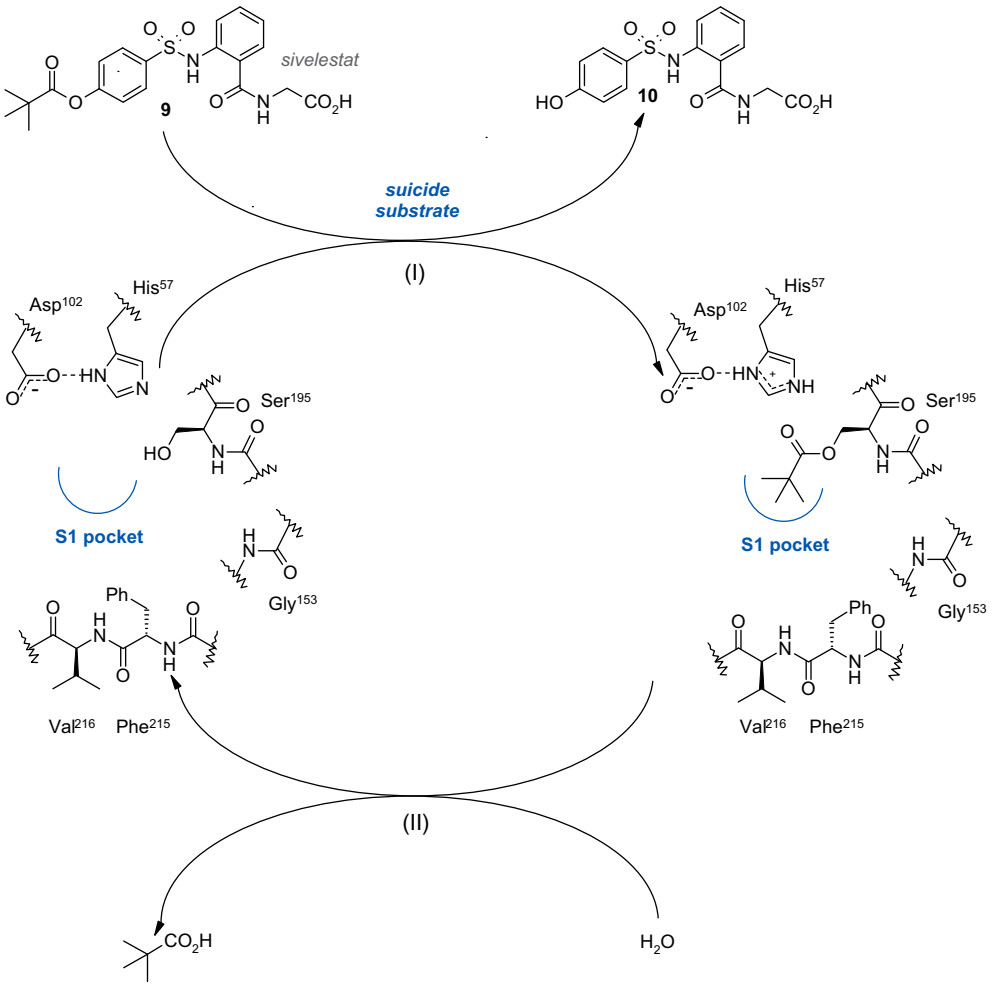

Figure 6. Reactive mode of action of sivelestat free acid **9**: (I) In the first step sivelestat free acid, acetylates Ser[195]; (II) concomitant hydrolysis again frees up Ser[195] (modified according to Ref. 38,39).

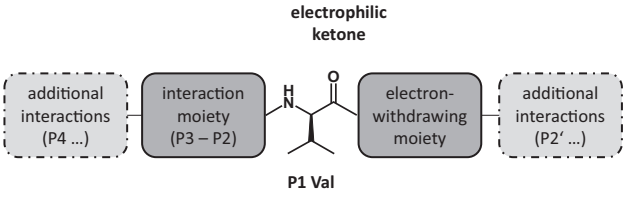

Figure 7. Modular features of reactive, 2nd generation neutrophil elastase inhibitors (modified according to Ref. 42).

potent, and orally bioavailable candidates AZD9668 (alvelestat, **13**) and BAY-678 (**17**) have entered clinical testing.

Both clinical candidates AZD9668 (**13**) and BAY-678 (**17**) contain an identical S1 binding motif [*m*-(trifluoromethyl)phenyl]. An X-ray structure of HNE-bound **12** (a close congener of **13**) has surprisingly revealed that this S1 binding motif in conjunction with the central pyridone scaffold apparently widens the *remote* S2 pocket significantly (Fig. 11). In the case of **18** (a close congener of **17**), the enlarged S2 pocket is perfectly filled with the *p*-cyanophenyl moiety (Fig. 12). More elaborate molecules with additional target interactions show an even improved (subnanomolar) potency relative to the clinical candidates: namely, congeners of AZD9668 (**13**) with an additional S2 binding motif, such as **15** (*p*-cyanophenyl), or congeners of BAY-678 (**17**) with additional potential contacts along the S′ substrate binding cleft, such as **19** (carboxylic acid side chains).[57] These modern inhibitors have displayed an outstanding selectivity versus similar serine proteases and a very high target specificity with no significant interactions with other pharmaceutically relevant targets, in contrast to 2nd generation inhibitors such as the potent, orally bioavailable, but *reactive* clinical candidate ONO-6818 (**8**, freselestat).[59]

AZD9668 (**13**) and BAY-678 (**17**) have revealed significant efficacy in preclinical models of ALI and lung emphysema, demonstrating their anti-inflammatory and anti-remodeling mode of action. Additionally, BAY-678 (**17**) has shown significant beneficial pulmonary hemodynamic and vascular effects in models of PAH in rats and mice.[61–63]

The safety and efficacy of AZD9668 (**13**) and BAY-678 (**17**) have been initially assessed in clinical Phase I trials with healthy volunteers and with COPD patients. All these trials have confirmed a very good safety and tolerability of these two 3rd and 4th generation elastase inhibitors. Both compounds are suitable for a chronic twice daily oral administration.[64] Noteworthy, the clinical development of the 2nd generation inhibitor ONO-6818 (**8**) has been discontinued due to abnormal elevation of liver function test values.[65] BAY-678 (**17**) is nominated as a chemical probe to the public via the Structural Genomics Consortium (SGC).[66]

From bench to bedside: Although HNE is an accepted target in the scientific community, the inhibition of the enzyme remains an innovative approach from the clinical perspective. There is still

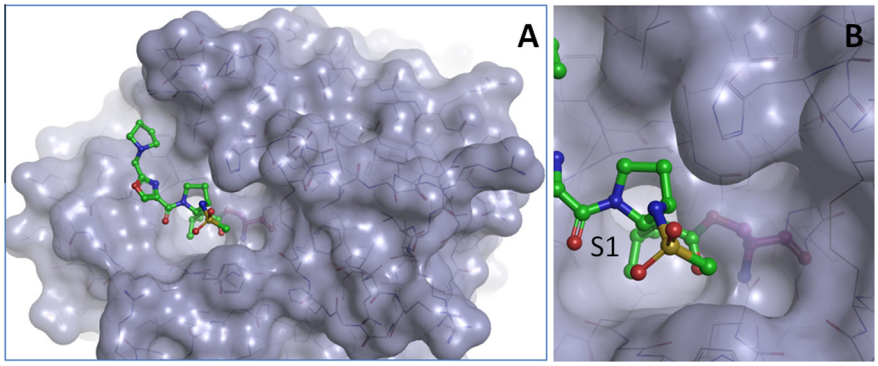

Figure 8. Crystal structure of HNE in complex with 2nd generation *trans*-lactam inhibitor GW475151 (**3**) a close congener of GW311616A (**2**) (PDB entry 1H1B): The protease is shown in a stick representation with transparent Connolly-like surface; ligand **3** (green) is shown as balls and sticks. Heteroatoms are colored as follows: oxygen, red; nitrogen, blue; sulfur, yellow. (A) View from above into the substrate binding cleft of HNE with deep S1 pocket; (B) detailed view of the covalent binding of the reactive *N*-methanesulfonyl-lactam moiety of the inhibitor (bright ball and sticks) to Ser^{195} (chymotrypsin numbering) of HNE (dark ball and sticks).

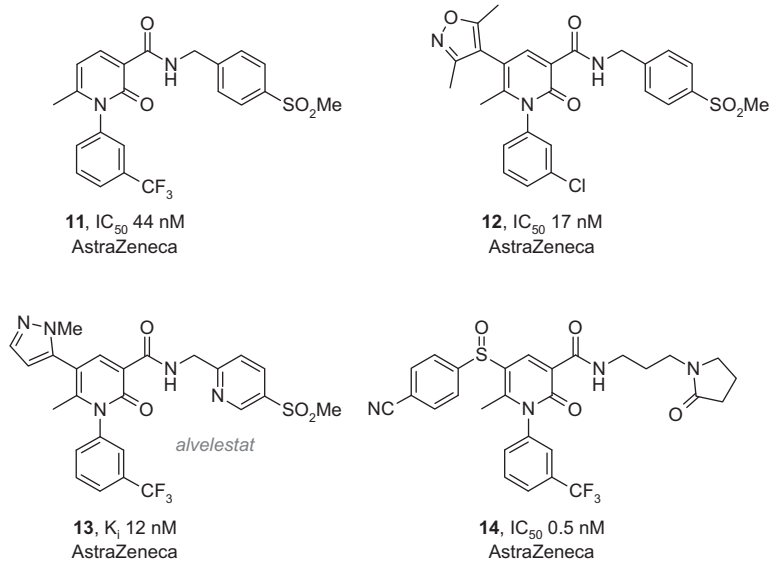

11, IC_{50} 44 nM
AstraZeneca

12, IC_{50} 17 nM
AstraZeneca

13, K_i 12 nM
AstraZeneca

14, IC_{50} 0.5 nM
AstraZeneca

Figure 9. Selection of 3rd generation neutrophil elastase inhibitors (SMOLs, nonreactive and reversible): alvelestat (**13**) is in Phase II trials (COPD, CF, BE). Early pyridones **11**–**14** only occupy the S1 pocket of HNE (see Fig. 11).

no sound guidance as to the degree elastase has to be inhibited to show beneficial clinical effects. Furthermore, it is not clear whether a sole inhibition of elastase will have a meaningful effect in patients. In a base case scenario, the aim might be a 50–90% inhibition range of elastase to foster (presumably) beneficial clinical effects without potentially hampering the innate immune response function of the target.

Besides traditional human dose estimates based on experimental pharmacology and drug metabolism and pharmacokinetics (DMPK) data, an additional attractive tool might be elastase activity assessment in human plasma after an ex vivo zymosan challenge in whole blood. Here, the yeast cell wall component zymosan is applied ex vivo in whole blood to activate resting neutrophils and thereby to elicit a sterile inflammation comprised of the typical morphological change of the neutrophil cells and the exhaustive depletion of the HNE-bearing granula.[67] In contrast to in vitro tests which in general apply isolated, highly purified neutrophil elastase, this ex vivo test makes use of neutrophil cells as the source for in situ liberated elastase molecules. Thus, the ex vivo conditions integrate many more features of the complex (patho)physiological conditions present in a neutrophil-driven inflammation in vivo than any in vitro test could incorporate, including: (1) the presence of antiproteases in whole blood reflecting the endogenous protection shield (protease–antiprotease balance), (2) the presence of other plasma proteins and components (e.g., albumin), and (3) oxidative stress conditions during neutrophil activation.

When this procedure was applied after oral administration of the drug in healthy volunteers and in COPD patients, AZD9668 (**13**) displayed a dose-dependent ex vivo inhibition of neutrophil elastase in whole blood around C_{max} values (1–4 h). However, at 24 h, only one dose (60 mg twice daily) revealed a relevant inhibitory capacity with approximately 50% inhibition. Higher doses did not translate into a higher target inhibition at 24 h, although C_{max} and AUC (0–24 h) were dose-proportional over the entire dose range. The reason for this is not known; it might be surmised and speculated that AZD9668 (**13**) is not sufficiently stable, for example, under sustained oxidative stress conditions.[68] Based on these data, a dose of 60 mg b.i.d. AZD9668 (**13**) has been orally administered to assess safety and efficacy in CF, BE, and COPD patients.

In these clinical Phase II studies, AZD9668 (**13**) was safe and well tolerated. Besides some promising results in a small study with BE patients or in a subgroup of a larger COPD trial, in general

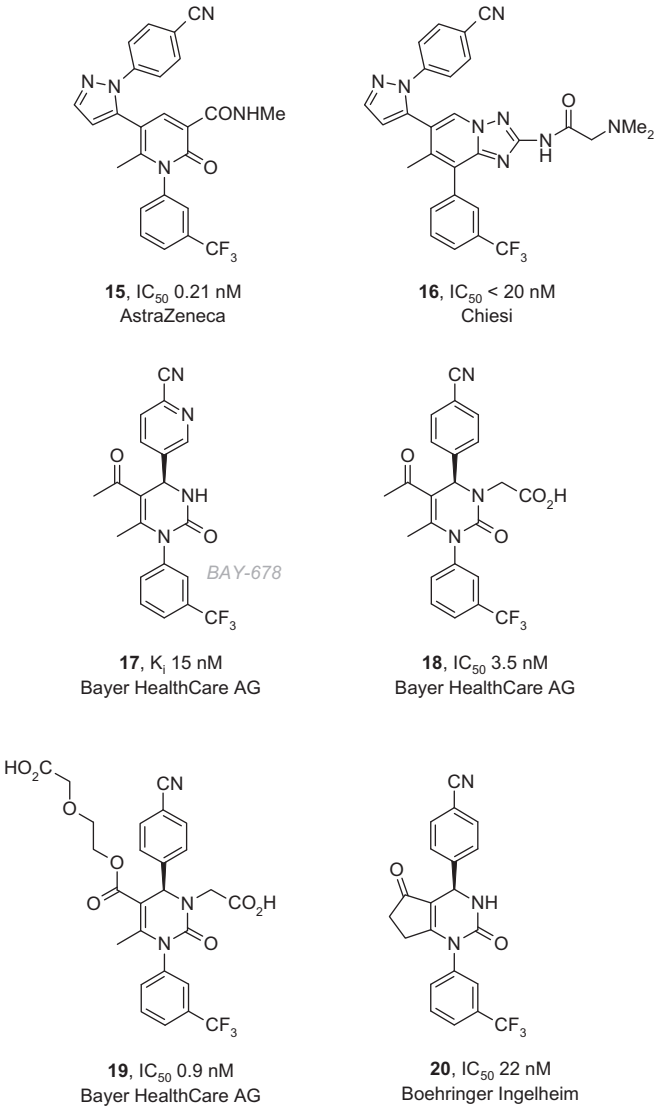

Figure 10. Selection of 4th generation neutrophil elastase inhibitors (SMOLs, nonreactive and reversible, addressing the S1 and the S2 pocket of HNE): BAY-678 (**17**) reached Phase I trials (COPD). Pyrimidinones **17**–**19** and also highly elaborated pyridones such as **15** are the key classes. In addition, further related series including cyclopentenone analogues such as **20** or triazolopyridines such as **16**[58] have been described.

a robust primary clinical efficacy could not be demonstrated (e.g., lung function parameters and quality of life). However, some promising effects with regard to secondary outcome parameters, such as inflammatory or mechanistic biomarkers, were seen.[68–71] Most probably, the treatment duration in these studies was too short for a disease-modifying treatment (4-week and 12-week treatment in BE/CF and COPD patients, respectively) to expect significant changes in the primary clinical objectives.[72] Recently published data for the cytokine receptor CXCR2 antagonist MK-7123 in a 26-week dose-finding study in COPD patients revealed a significant effect on neutrophil sputum count and some effects on inflammatory biomarkers after 12 weeks; however, effects on lung function were only demonstrated after 26 weeks.[73] There were no effects on the rate of exacerbations. Apparently, an even longer study duration is necessary to demonstrate efficacy concerning exacerbations, as shown with the two 1-year trials with the phosphodiesterase PDE4 inhibitor roflumilast in COPD patients.[74,75]

AZD9668 (**13**) is currently available within AstraZeneca's open innovation initiative.

BAY-678 (**17**) has not entered Phase II trials due to a switch to a significantly improved follow-up HNE inhibitor, BAY 85-8501 (**22**) (see 5th generation HNE inhibitors).

5th generation (pre-adaptive pharmacophores derived from 4th generation inhibitors): The 5th generation of neutrophil elastase inhibitors are structurally closely related to the 4th generation inhibitors. However, in the 5th generation inhibitors (Fig. 13), an additional substituent results in an unprecedented improvement in potency though it does not directly interact with the target. In fact, the additional substituent (e.g., SO_2Me in **21**, Fig. 14)[76] raises the rotational barrier at the crucial pyrimidinone-cyanophenyl axis and thereby 'freezes' the structure in an ideal bioactive conformation, thus pre-organizing the inhibitor for the forthcoming binding event. Remarkably, in this case the spatial change that will happen within the target enzyme-upon the induced-fit binding process is conformationally pre-empted by the inhibitor (*pre-adaptive pharmacophore model*).[77]

For example, BAY 85-8501 (**22**) displays an extraordinary potency (K_i 0.08 nm), already comparable to the endogenous antiproteases and remarkable two orders of magnitude higher when compared with corresponding 4th generation inhibitors (Table 2). Furthermore, the in vitro inhibitory capacity of BAY 85-8501 is maintained in the presence of 1 mm H_2O_2 (mimicking oxidative stress conditions, data for other inhibitors not published). This leap in potency comes with increased selectivity towards other serine proteases: Most serine proteases show less

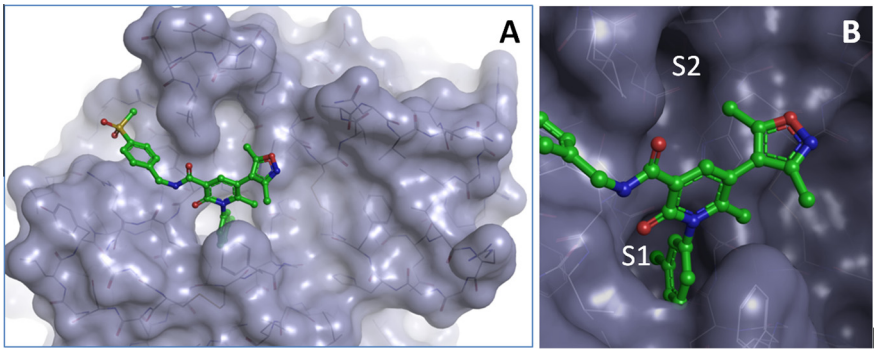

Figure 11. Crystal structure of HNE in complex with 3rd generation inhibitor **12** (in house data, PDB entry 5abw),[60] a close congener of AZD9668 (**13**): The protease is shown in a stick representation with transparent Connolly-like surface (grey); ligand **12** (green) is shown as balls and sticks. Heteroatoms are colored as follows: oxygen, red; nitrogen, blue; chlorine, dark green; sulfur, yellow. (A) View from above into the substrate binding cleft of HNE; compound **12** binds into the S1 pocket, the formation of the *de novo* deep S2 pocket is induced but not fully filled with the small methyl moiety of the inhibitor, the *p*-methylsulfonyl moiety binds into the S4 pocket; (B) detailed side view of the noncovalent, induced-fit binding moiety of compound **12** perfectly filling the S1 pocket and pointing towards the *de novo* deep S2 pocket. (See Fig. 15A for the presumed binding geometry of a 4th generation inhibitor of this series, namely **15**.)

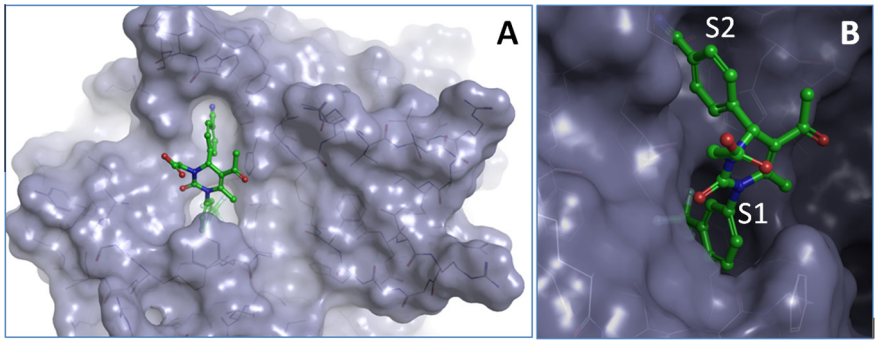

Figure 12. Crystal structure of HNE in complex with 4th generation inhibitor **18**, a close congener of BAY-678 (**17**) (PDB entry 5a09): The protease is shown in a stick representation with transparent Connolly-like surface (grey); ligand **18** (green) is shown as balls and sticks. Heteroatoms are colored as follows: oxygen, red; nitrogen, blue; fluorine, light green. (A) View from above into the substrate binding cleft of HNE with deep S1 pocket and *de novo* formed S2 pocket, the inhibitor binds in an almost perpendicular orientation; (B) detailed side view of the noncovalent, induced-fit binding of compound **18** perfectly filling the S1 pocket and the *de novo* formed, deep S2 pocket.

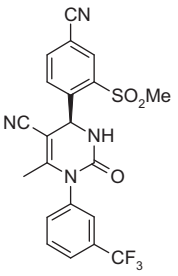

21, IC_{50} < 0.3 nM
Bayer HealthCare AG

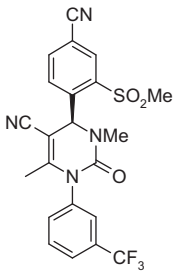

22, K_i 0.08 nM
Bayer HealthCare AG

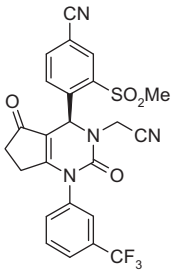

23, IC_{50} < 1 nM
Boehringer Ingelheim

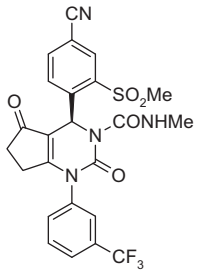

24, IC_{50} < 1 nM
Boehringer Ingelheim

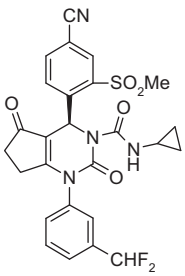

25, IC_{50} < 1 nM
Boehringer Ingelheim

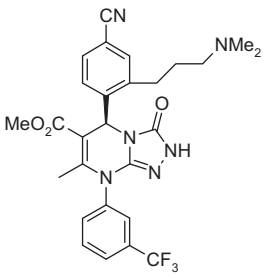

26, IC_{50} < 20 nM
Chiesi

Figure 13. Selection of 5th generation neutrophil elastase inhibitors (SMOL with pre-adaptive pharmacophore); BAY 85-8501 (**22**) is currently in a Phase II trial (BE). Again, annulated variants of the pyrimidinone core, such as triazolopyrimidines (e.g., **26**), have been prepared.[78]

than 40% identity with respect to their primary sequence but share the typical overall fold of serine proteases with very similar active-site geometries. Here, an unprecedented selectivity of more than five orders of magnitude is reached with **22** (Table 3). A selectivity of almost two orders of magnitude has even been demonstrated for a few proteases sharing a high primary sequence identity with HNE, for example, orthologous neutrophil elastase from rats or mice, and proteinase 3 (PR3) with approximately 70% primary sequence identity (no proteinase 3 inhibition data published for BAY 85-8501).

Compared to the overall promising rodent DMPK profile of the 3rd and 4th generation inhibitors, BAY 85-8501 (**22**) shows a further improved metabolic stability translating into a low clearance and improved half-life with no inhibitory capacity towards CYP isoforms.[76] Studies with BAY 85-8501 (**22**) have confirmed an anti-inflammatory and anti-remodeling mode of action in preclinical acute and chronic animal models of ALI, PAH, and PH associated with lung emphysema.[76,80–82]

Recently, more research groups from industry have been attracted to 5th generation inhibitors, leading to further improvements in potency and metabolic stability (**23**–**25**, Table 4; Fig. 15).[83,84]

Compromising the host defense of patients has been discussed as a hypothetical side effect of elastase inhibition. However, the intrinsic risk of the 3rd, 4th, and 5th generation HNE inhibitors to interfere with the host defense should be regarded as being low because the intracellular elastase concentration is very high (millimolar concentration range) and a potential accumulation of HNE-bound inhibitors upon chronic treatment is unlikely due to their nonreactive and reversible mode of action.

Clinical Phase I studies have been conducted with healthy male volunteers to evaluate safety, tolerability, and pharmacokinetics of once daily, orally administered BAY 85-8501 (**22**). In all studies, the drug was safe and well tolerated at single and multiple doses (tested up to 1 mg) without evidence of adverse effects related to the drug or its mechanism of action. Exposure to BAY 85-8501 (**22**) increased proportionally with dose, approaching steady state at 14 days with a half-life of 120–140 h. Renal elimination of unchanged drug is only a minor pathway for elimination. Thus, special precautions for the potential treatment of renal-impaired patients are not expected. Inhibition of neutrophil elastase activity in plasma after ex vivo zymosan challenge in whole blood was reversible, occurred in a dose-dependent manner over the entire dosing interval, and correlated well with the drug exposure. At steady state, IC_{50} was covered with a dose >0.6 mg, while IC_{90} was covered with the 1-mg dose.[85–87]

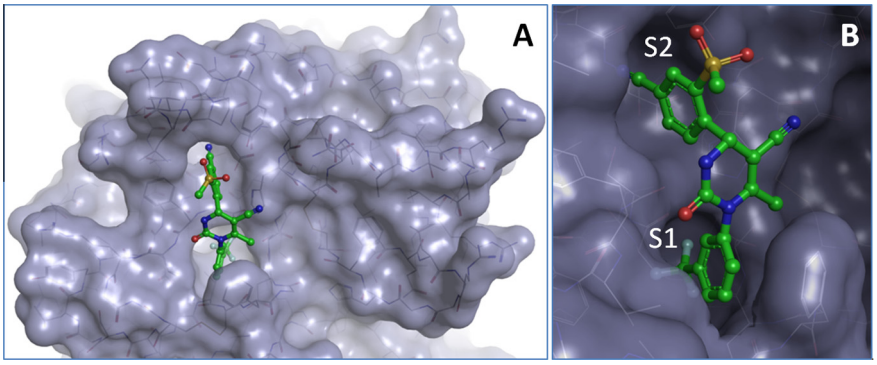

Figure 14. Crystal structure of HNE in complex with 5th generation inhibitor **21**, a close congener of BAY 85-8501 (**22**) (PDB entry 5a0c): The protease is shown in a stick representation with transparent Connolly-like surface (grey); ligand **21** (green) is shown as balls and sticks. Heteroatoms are colored as follows: oxygen, red; nitrogen, blue; fluorine, light green; sulfur, yellow. (A) View from above into the substrate binding cleft of HNE with deep S1 pocket and *de novo* formed S2 pocket, C2′–SO_2Me points towards the solvent without any target interaction; (B) detailed side view of **21** perfectly matching the induced-fit target binding geometry. [See Fig. 15B for the presumed binding geometry of BAY 85-8501 (**22**).]

Table 2
Potency of selected examples of HNE inhibitors

	1st generation		2nd generation		3rd generation	4th generation	5th generation
	α-1 PI[77]	Elafin[77]	ONO-5046 (**7**)[45]	ONO-6818 (**8**)[42]	AZD9668 (**13**)[59]	BAY-678 (**17**)[76]	BAY 85-8501 (**22**)[76]
K_i (nm)	<0.1	0.08	200	12	12	15	0.08

Table 3
Selectivity of selected examples of HNE inhibitors (reported as ratio of IC_{50} or K_i against the protease of interest versus the value against HNE; *based on on-rates)

Protease	1st generation		2nd generation		3rd generation	4th generation	5th generation
	α-1 PI[78]	Elafin[78]	ONO-5046 (**7**)[59]	ONO-6818 (**8**)[59]	AZD9668 (**13**)[59]	BAY-678 (**17**)[76]	BAY 85-8501 (**22**)[76]
HNE	1*	1*	1	1	1	1	1
PR3	8*	1*	3	63	>1900	600	—
CatG	160*	—	>2000	>2000	>680	>660	>375000
Chymotrypsin	—	—	199	1000	>2000	>660	>375000
Pancreatic elastase	—	—	79	79	>2000	>660	>375000
Trypsin	—	—	>2000	>2000	>2000	>660	>375000
Rat NE	—	—	1.1	—	18	40	100
Murine NE	—	—	0.4	—	24	47	75

Table 4
Comparison of potency, half-life, and clearance of the 4th generation inhibitor **20** and derived 5th generation inhibitor derivatives **23**–**25**[84]

HNE inhibitor	HNE plasma assay IC_{50} (nm)	Human hepatocytes half-life (min)	Predicted human hepatic in vivo blood clearance CL (mL/min/kg)
20	22	>130	6
23, **24**, **25**	<1	>130	0

Consequently, a dose of 1 mg (orally once daily treatment) was selected to initially assess the safety of BAY 85-8501 (**22**) in patients and to evaluate efficacy. Here, a 4-week clinical Phase II study with 92 NCF BE patients (NCT No. 01818544, study completed with no results published so far) was conducted with a design resembling the exploratory trial with AZD9668 (**13**) (vide supra).

Further neutrophil elastase inhibition principles: Peptidic inhibitors and gene therapy: The design of peptidic inhibitors combines the

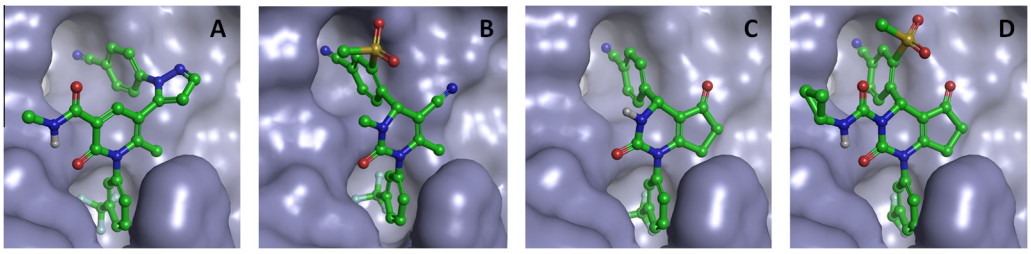

Figure 15. Overview of the active site of HNE structure (PDB entry 5a0c) with superimposed ligands in order to display the prooven and/or presumed binding geometries. (A–D): **15**,[57] **22**,[76] **20**,[84] and **25**.[79] As a common feature all these 4th and 5th generation inhibitors clamp the S1 and S2 pocket. Notably, the pyridone **15** manages to reach the S2 pocket with its *para*-cyanophenyl residue via a pyrazole 'joint' (A). In contrast, within the entire pyrimidinone series, diving into the S2 pocket is possible with *para*-cyanophenyl residues that are directly attached to the central scaffold (B and C).

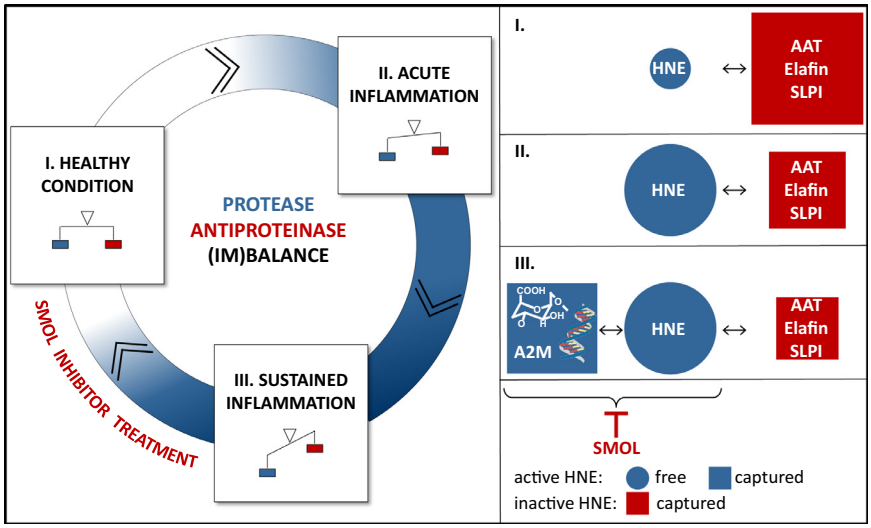

Figure 16. Schematic representation of the protease–antiprotease (im)balance and the subsequent partition of free and captured HNE; in (III), binding to alpha-2 macroglobulin (A2M) and polyanionic surfaces, for example, DNA filaments in NETosis (helix symbol) and heparan sulfates (carbohydrate symbol); the size of the circles/squares reflects the relative amounts of free/captured elastase (not proportional). A SMOL inhibitor could potentially shift the system from sustained inflammation (III) to a more healthy stage (I).

idea of the *Lock and Key Model* with the *Pharmacophore Model* to create 'hybrid' 1st/2nd generation inhibitors. However, peptides often suffer from a poor pharmacokinetic profile and none of the linear or cyclic elastase inhibitory peptides derived from phage display campaigns has turned out to be a drug-like molecule allowing clinical testing. The situation seems to be better for the β-hairpin peptide POL6014 that might enter clinical testing in the future following a strict inhaled administration protocol. Start of clinical phase 1 testing is planned in 2015.[88] This peptide has been discovered with a so-called protein epitope mimetic (PEM) technology starting from a natural β-hairpin-bearing, reactive-site loop of the Bowman–Birk family of serine proteases.[89,90] Derivatization of this loop motif occurred via the exchange of building blocks in a solid-phase synthesis which enabled the generation of a peptide library in a combinatorial-chemistry-like manner, including non-proteinogenic amino acids or unrelated building blocks. The structure of POL6014 is yet to be disclosed including further information on whether POL6014 still bears the disulfide bridge of the natural template. Nebulized POL6014 revealed preclinical efficacy in ALI models and concentration in the lungs was 100-fold higher than in plasma.[91–93]

A variation of the augmentation therapy (1st generation inhibitors) has been used to treat patients with the DNA 'blueprint' of the antiprotease rather than with the protein itself. In general, these gene therapy treatment efforts face the issue of a sufficient and controlled delivery of the DNA-bearing vector to the tissue of interest. First clinical attempts are underway.[94–96] Another variation to interfere with the protease–antiprotease imbalance applies RNA interference strategies (e.g., shRNA and miRNA) which have only been explored preclinically so far.[95]

Outlook: Challenges and opportunities: Disease-modifying therapies for the aforementioned pulmonary diseases are innovative from the clinical perspective as the medical need for such treatments is very high. One big challenge is that a disease-modifying therapy with an anti-inflammatory and anti-remodeling treatment will potentially not have an immediate impact on relevant clinical parameters (e.g., lung function and quality-of-life scores) compared to a symptomatic therapy (e.g., bronchodilator treatment). Consequently, clinical trials with significantly longer treatment durations will probably have to be conducted to achieve a proof-of-concept. In particular, this is the case for exacerbation rates.[97] Furthermore, a direct demonstration of an anti-remodeling treatment effect likely demands a patient cohort with a minor disease severity to better monitor the progression of the disease (longitudinal evaluation of high-resolution computed tomography scans, HRCT), presumably resulting in even longer clinical trials. Such trials are typically risky and expensive.

A neutrophil elastase inhibitor treatment in a clinical setting needs to take into account the protease–antiprotease imbalance in the respective disease. In general, an area of obligate HNE activity exists around activated neutrophils where the local concentration of the liberated elastase is higher than the apparent concentration of the antiproteases (see introduction and Fig. 1). This general scenario is reflected in the ex vivo testing of neutrophil elastase activity after zymosan challenge in whole blood samples (see 3rd, 4th, and 5th generation inhibitors).

However, the spatiotemporal dimensions of this area might be larger at the pathophysiological sites in diseased tissue (with sustained inflammation) where the partition of the active protease and effective antiprotease might be different to the situation in a *de novo* inflammation (in situ elicited inflammation). In certain pathophysiological conditions, active elastase is captured in competing 'micro-compartments' circumventing an efficient neutralization by antiproteases (Fig. 16). For example, similar to the situation of elastase embedded in the neutrophil membrane, the active protease is partially protected from the antiprotease upon binding to alpha-2 macroglobulin or polyanionic binding partners such as (1) heparan sulfate components of syndecan-1 in the sputum of BE patients,[98,99] and (2) nucleic acid filaments in neutrophil extracellular traps of dying neutrophils (NETosis) in sputum and blood samples of patients with BE, CF, tuberculosis, and sepsis.[100,101] Thus, not only neutrophil elastase derived from freshly activated neutrophils, but also that derived from the 'debris' of previously engaged neutrophil cells, will contribute to the overall elastase activity which is not adequately addressed by the antiproteases.[102] Furthermore, the inhibitory capacity of the antiproteases is hampered in certain pathophysiological conditions. For example, bacteria are not effectively cleared from the airways of CF or BE patients and bacterial proteases could degrade the antiproteases. Environmental (tobacco smoke, air pollution) or genetic (AATD) factors could further decrease the effective antiprotease concentration in patients.[103] The partition is further influenced by a different

vulnerability of the three major antiproteases (α-1 PI, SLPI, elafin) towards oxidation and affinity towards the three major neutrophil serine proteases (HNE, CatG, PR3).[79,104,105] To date, it is still uncertain how high the spatiotemporal concentration of active elastase (and other proteases) really is in such disease settings!

Thus, aiming for a 50–90% inhibition of elastase, the necessary dose for a clinical elastase inhibitor treatment might be higher than the estimated dose based on ex vivo whole blood testing or preclinical models which, in general, do not reflect any mucus-ridden airways/lungs. Noteworthy, the dose of AZD9668 (**13**, 60 mg b.i.d.) in clinical testing was close to the 70 mg b.i.d. limit based on preclinical toxicological data, which does not allow for a significant further dose escalation.[64,71]

Nevertheless, neutrophil elastase inhibitors of the 5th generation bear the potential to overcome at least some of these challenges in order to re-establish the protease–antiprotease balance in patients. Their higher potency and selectivity should allow for higher daily doses due to a presumably better safety profile. Hopefully this will stimulate multiple players in the field to enter extended proof-of-concept clinical trials in disease modifying treatment regimens. These treatments might be applied in conjunction with other therapies such as DNAse, mucolytics, antibiotics, and tobacco dehabituation. In addition, easy access to chemical tools such as AZ9668 (**13**) and BAY-678 (**17**) should further support many labs investigating the important biology of HNE in multiple disease settings.

Acknowledgments

We thank Jens Schamberger and Martina Schäfer for scientific support with docking studies and the interpretation of X-ray data. We thank Ines Bohlinger for help with the patent literature. Valuable discussions with Susanne Wegner, Tiemo-Jörg Bandel and Johannes Nagelschmitz about clinical studies were very helpful. We are grateful to Sandra Korthals and Kay Greenfield for technical support with the manuscript.

References and notes

1. Bardoel, B. W.; Kenny, E. F.; Sollberger, G.; Zychlinsky, A. *Cell Host Microbe* **2014**, *15*, 526.
2. Stockley, R. A. *Am. J. Respir. Crit. Care Med.* **1999**, *160*, S49.
3. Lee, W. L.; Downey, G. P. *Am. J. Respir. Crit. Care Med.* **2001**, *164*, 896.
4. Cech, P.; Lehrer, R. I. *Blood* **1984**, *63*, 88.
5. Cowburn, A. S.; Condliffe, A. M.; Farahi, N.; Summers, C.; Chilvers, E. R. *Chest* **2008**, *134*, 606.
6. Stockley, R. A. *Chest* **2002**, *121*, 151S.
7. Liou, T. G.; Campbell, E. J. *Biochemistry* **1995**, *34*, 16171.
8. Liou, T. G.; Campbell, E. J. *J. Immunol.* **1996**, *157*, 2624.
9. Brinkmann, V.; Zychlinsky, A. *Nat. Rev. Microbiol.* **2007**, *5*, 577.
10. Hickey, M. J.; Kubes, P. *Nat. Rev. Immunol.* **2009**, *9*, 364.
11. Laurell, C. B.; Eriksson, S. *Scand. J. Clin. Lab. Invest.* **1963**, *15*, 132.
12. Shapiro, S. D.; Goldstein, N. M.; Houghton, A. M.; Kobayashi, D. K.; Kelley, D.; Belaaouaj, A. *Am. J. Pathol.* **2003**, *163*, 2329.
13. Chua, F.; Dunsmore, S. E.; Clingen, P. H.; Mutsaers, S. E.; Shapiro, S. D.; Segal, A. W.; Roes, J.; Laurent, G. J. *Am. J. Pathol.* **2007**, *170*, 65.
14. Zaidi, S. H. E.; You, X.-M.; Ciura, S.; Husain, M.; Rabinovitch, M. *Circulation* **2002**, *105*, 516.
15. Zaidi, S. H. E.; Hui, C.-C.; Cheah, A. Y. L.; You, X.-M.; Husain, M.; Rabinovitch, M. *J. Clin. Invest.* **1999**, *103*, 1211.
16. Belaaouaj, A.; McCarthy, R.; Baumann, M.; Gao, Z.; Ley, T. J.; Abraham, S. N.; Shapiro, S. D. *Nat. Med.* **1998**, *4*, 615.
17. Jiang, D.; Persinger, R.; Wu, Q.; Gross, A.; Chu, H. W. *Respir. Res.* **2013**, *14*, 122.
18. Jiang, D.; Wenzel, S. E.; Wu, Q.; Bowler, R. P.; Schnell, C.; Chu, H. W. *PLoS One* **2013**, *8*, e64689.
19. Lucas, S. D.; Costa, E.; Guedes, R. C.; Moreira, R. *Med. Res. Rev.* **2013**, *33*, E73.
20. Stockley, R. A. *Expert Opin. Emerging Drugs* **2010**, *15*, 685.
21. Stockley, R. A. *Clin. Chest Med.* **2014**, *35*, 39.
22. Sallenave, J. M. *Am. J. Respir. Cell Mol. Biol.* **2010**, *42*, 635.
23. Guyot, N.; Butler, M. W.; McNally, P.; Weldon, S.; Greene, C. M.; Levine, R. L.; O'Neill, S. J.; Taggert, C. C.; McElvaney, N. G. *J. Biol. Chem.* **2008**, *283*, 32377.
24. Nobar, S. M.; Zani, M. L.; Boudier, C.; Moreau, T.; Bieth, J. G. *FEBS J.* **2005**, *272*, 5883.
25. Beatty, K.; Bieth, J.; Travis, J. *J. Biol. Chem.* **1980**, *255*, 3931.
26. Taggart, C.; Cervantes-Laurean, D.; Kim, G.; McElvaney, N. G.; Wehr, N.; Moss, J.; Levine, R. L. *J. Biol. Chem.* **2000**, *275*, 27258.
27. Chotirmall, S. H.; Al-Alawi, M.; McEnery, T.; McElvaney, N. *Ther. Clin. Risk Manage.* **2015**, *11*, 143.
28. Owen, C. A.; Campbell, M. A.; Sannes, P. L.; Boukedes, S. S.; Campbell, E. J. *J. Cell Biol.* **1995**, *131*, 775.
29. Huntington, J. A.; Randy, J. R.; Carrell, R. W. *Nature* **2000**, *407*, 923.
30. Proteo Biotech AG Press Releases 23rd February 2011; http://proteo.de/pages/12/press-releases/2011/02/23/elafin-shortens-intensive-care-after-surgery-for-esophagus-cancer/ and 8th November 2013; http://proteo.de/pages/press/press-releases/2013/11/08/patient-recruitment-and-treatment-in-elafin-cabg-phase-ii-clinical-trial-completed/; accessed 20th May, 2015.
31. Clinicaltrials.gov NCT study code NCT01394835.
32. Clinicaltrials.gov NCT study code NCT01523821.
33. Clinicaltrials.gov NCT study code NCT01700036.
34. Clinicaltrials.gov NCT study code NCT01936896.
35. Clinicaltrials.gov NCT study code NCT02191839.
36. Metz, W. A.; Peet, N. P. *Expert Opin. Ther. Pat.* **1999**, *9*, 851.
37. Skiles, J. W.; Jeng, A. Y. *Expert Opin. Ther. Pat.* **1999**, *9*, 869.
38. Ohbayashi, H. *Expert Opin. Invest. Drugs* **2002**, *11*, 965.
39. Nakayama, Y.; Odagaki, Y.; Fujita, S.; Matsuoka, S.; Hamanaka, N.; Nakai, H.; Toda, M. *Bioorg. Med. Chem. Lett.* **2002**, *12*, 2349.
40. Ishiyama, J.; Araki, K.; Miura, M. P.; Kitamura, Y.; Izawa, S.; Okerberg, E. S. et al. *Abstract of Papers*, 237th National Meeting of the American Chemical Society, Washington, DC, 2009; Abstract 195.
41. McDonald, S. J.; Dowle, M. D.; Harrison, L. A.; Clarke, G. D.; Inglis, G. C.; Johnson, M. R.; Shah, P.; Smith, R. A.; Amour, A.; Fleetwood, G.; Humphreys, D. C.; Molloy, C. R.; Dixon, M.; Godward, R. E.; Wonacott, A. J.; Singh, O. M.; Hodgson, S. T.; Hardy, G. W. *J. Med. Chem.* **2002**, *45*, 3878.
42. Odagaki, Y.; Ohmoto, K.; Matsuoka, S.; Hamanka, N.; Nakai, H.; Toda, M.; Katsuya, Y. *Bioorg. Med. Chem.* **2001**, *9*, 647.
43. Perone, J. J.; Craik, C. S. *Protein Sci.* **1995**, *4*, 337.
44. Bode, W.; Meyer, E.; Powers, J. C. *Biochemistry* **1951**, *1989*, 28.
45. Kawabata, K.; Suzuki, M.; Sugitani, M.; Imaki, K.; Toda, M.; Miyamoto, T. *Biochem. Biophys. Res. Commun.* **1991**, *177*, 814.
46. Watanabe, F.; Sato, M.; Kato, A.; Murakami, T.; Higashi, Y.; Yata, N. *Biol. Pharm. Bull.* **1997**, *20*, 392.
47. *Drugs Future* **1998**, *23*, 1254.
48. Tamakuma, S.; Ogawa, M.; Aikawa, N.; Kubota, T.; Hirasawa, H.; Ishizaka, A.; Taenaka, N.; Hamada, C.; Matsuoka, S.; Abiru, T. *Pulm. Pharmacol. Ther.* **2004**, *17*, 271.
49. Zeiher, B. G.; Matsuoka, S.; Kawabata, K.; Repine, J. E. *Crit. Care Med.* **2002**, *30*, S281.
50. Zeiher, B. G.; Artigas, A.; Vincent, J. L.; Dmitrienko, A.; Jackson, K.; Thompson, B. T.; Bernard, G. *Crit. Care Med.* **2004**, *32*, 1695.
51. Aikawa, N.; Kawasaki, Y. *Ther. Clin. Risk Manage.* **2014**, *10*, 621.
52. Miyoshi, S.; Hamada, H.; Ito, R.; Katayama, H.; Irifune, K.; Suwaki, T.; Nakanishi, N.; Kanematsu, T.; Dote, K.; Aibiki, M.; Okura, T.; Higaki, J. *Drug Des. Dev. Ther.* **2013**, *7*, 305.
53. Hansen, G.; Gielen-Haertwig, H.; Reinemer, P.; Schomburg, D.; Harrenga, A.; Niefind, K. *J. Mol. Biol.* **2011**, *409*, 681.
54. Oost, T.; Fiegen, D.; Gnamm, C. WO Patent 2014029830 A1, **2014**.
55. Oost, T.; Fiegen, D.; Gnamm, C.; Handschuh, S.; Peters, S.; Roth, G. J. WO Patent 2014029831 A1, **2014**.
56. Oost, T.; Fiegen, D.; Gnamm, C.; Handschuh, S.; Peters, S.; Roth, G. J. WO Patent 2014029832 A1, **2014**.
57. Sjö, P. *Future Med. Chem.* **2012**, *4*, 651.
58. Capaldi, C.; Heald, R. A.; Ray, N. C.; Sutton, J. M. WO Patent 201409425 A1, **2014** (Example 14).
59. Stevens, T.; Ekholm, K.; Gränse, M.; Lindahl, M.; Kozma, V.; Jungar, C.; Ottoson, T.; Falk-Håkansson, H.; Churg, A.; Wright, J. L.; Lal, H.; Sanfridson, A. *J. Pharmacol. Exp. Ther.* **2011**, *339*, 313.
60. Andersson, M.; Hansen, P.; Loenn, H.; Nikitidis, A.; Sjoelin, P. WO Patent 2005026123 A1, **2005** (Example 36).
61. Klein, M.; Kramer, F.; Golz, S.; von Nussbaum, F.; Kast, R.; Schäfer, S. *Eur. Heart J.* 2007, 28, *Abstract Suppl.:* 55. Abstract of Meeting Papers.
62. Klein, M.; Golz, S.; Li, V.; von Nussbaum, F.; Schäfer, S. *Clin. Res. Cardiol.* **2007**, *96*, Suppl. 1: P196. Abstract of Meeting Papers.
63. Klein, M.; Kramer, F.; Kast, R.; Schäfer, S. *Eur. Respir. J.* **2007**, Suppl. 7S. Abstract of Meeting Papers.
64. Gunawardena, K. A.; Gullstrand, H.; Perret, J. *Int. J. Clin. Pharmacol. Ther.* **2013**, *51*, 288.
65. Ono Pharmaceutical Co., Ltd Press Release 1st November 2002; https://www.ono.co.jp/eng/cn/contents/sm_cn_110102.pdf; accessed 20th May, 2015.
66. http://www.thesgc.org/.
67. Scher, J. U.; Abramson, S. B.; Pillinger, M. H. In *Kelley's Textbook of Rheumatology E-Book*; Firestein, G. S., Budd, R., Gabriel, S. E., O'Dell, J. R., McInnes, I. B., Eds., 9th ed.; Saunders, 2012; pp 152–169. Chapter 11.
68. Elborn, J. P.; Perret, J.; Forsman-Semb, K.; Marks-Konczalik, J.; Gunawardena, K. *Eur. Respir. J.* **2012**, *40*, 969.
69. Stockley, R.; De Soyza, A.; Gunawardena, K.; Perret, J.; Forsman-Semb, K.; Entwistle, N.; Snell, N. *Respir. Med.* **2013**, *107*, 524.
70. Kuna, P.; Jenkins, M.; O'Brien, C. D.; Fahy, W. A. *Respir. Med.* **2012**, *106*, 531.
71. Vogelmeier, C.; Aquino, T. O.; O'Brien, C. D.; Perret, J.; Gunawardena, K. *COPD* **2012**, *9*, 111.

72. Martinez-Garcia, M. A.; Soler-Cataluna, J. J.; Perpina-Tordera, M.; Roman-Sanchez, P.; Soriano, J. *Chest* **2007**, *132*, 1565.
73. Rennard, S. I.; Dale, D. C.; Donohue, J. F.; Kanniess, F.; Magnussen, H.; Sutherland, E. R.; Watz, H.; Lu, S.; Stryszak, P.; Rosenberg, E.; Staudinger, H. *Am. J. Respir. Crit. Care Med.* **2015**, *191*, 1001.
74. Calverly, P. M.; Sanchez-Toril, F.; McIvor, A.; Teichmann, P.; Bredenbroecker, D.; Fabbri, L. M. *Am. J. Respir. Crit. Care Med.* **2007**, *176*, 154.
75. Calverly, P. M.; Rabe, K. F.; Goehring, U. M.; Kristiansen, S.; Fabbri, L. M.; Martinez, F. J. *Lancet* **2009**, *374*, 685.
76. von Nussbaum, F.; Li, V.; Allerheiligen, S.; Anlauf, S.; Bärfacker, L.; Bechem, M.; Delbeck, M.; Fitzgerald, M. F.; Gerisch, M.; Gielen-Haertwig, H.; Haning, H.; Karthaus, D.; Lang, D.; Lustig, K.; Meibom, D.; Mittendorf, J.; Rosentreter, U.; Schäfer, M.; Schäfer, S.; Schamberger, J.; Telan, L. A.; Tersteegen, A. *ChemMedChem* **2015**, *10*, 1163.
77. Term chosen by analogy to 'adaptive mutation' in evolutionary biology. Cairns, J.; Overbaugh, J.; Miller, S. *Nature* **1988**, *335*, 142.
78. Alcaraz, L.; Heald, R. A.; Sutton, J. M.; Armani, E.; Capaldi, C. WO Patent 2014095700 A1, **2014** (Example 12).
79. Korkmaz, B.; Moreau, T.; Gauthier, F. *Biochimie* **2008**, *90*, 227.
80. Delbeck, M.; Li, V.; von Nussbaum, F.; Meibom, D.; Golz, S.; Lustig, K.; Trübel, H.; Schäfer, S. *Eur. Respir. J.* **2014**, *44,* Suppl. 58: P2352. Abstract of Meeting Papers.
81. Delbeck, M.; Micus, S.; Li, V.; von Nussbaum, F.; Meibom, D.; Lustig, K.; Trübel, H.; Schäfer, S. *Eur. Respir. J.* **2014**, *44,* Suppl. 58: 3424. Material presented orally.
82. Anlauf, S.; Freundlieb, J.; Gerisch, M.; Harrenga, A.; Himmel, H.; Karthaus, D.; Kerm, A.; Klein, M.; Kroh, W.; Krenz, U.; Lang, D.; Li, V.; Lustig, K.; Meibom, D.; Mittendorf, J.; von Nussbaum, F.; Schäfer, M.; Schäfer, S.; Schamberger, J.; Wegener, S. Presented at EFMC-ISMC 2014, Lisbon, September 2014; lecture LE096; *ChemMedChem* EFMC-ISMC 2014, 73. Material presented orally.
83. Abdel-Magid, A. F. *ACS Med. Chem. Lett.* **2014**, *5*, 1182.
84. Gnamm, C.; Oost, T.; Peters, S. U.S. Patent 20140221335 A1, **2014**.
85. Nagelschmitz, J.; Becka, M.; van der Mey, D.; Schwers, S.; von Nussbaum, F.; Li, V.; Wensing, G. *Eur. Respir. J.* **2014**, *44,* Suppl. 58: P1510. Abstract of Meeting Papers.
86. Nagelschmitz, J.; Becka, M.; van der Mey, D.; Schwers, S.; Wensing, G. *Eur. Respir. J.* **2014**, *44,* Suppl. 58: P1511. Abstract of Meeting Papers.
87. Nagelschmitz, J.; Kaufel, D.; Schwers, S.; von Nussbaum, F.; Li, V.; Delbeck, M.; Lustig, K.; Bandel, T.; Watz, H. *Eur. Respir. J.* **2014**, *44,* Suppl. 58: 3416. Material presented orally.
88. Polyphor Ltd, Press Release 9th January 2015; http://www.polyphor.com/assets/files/Press_Release/Polyphor-PARI_press%20release_final.pdf; accessed 20th May, 2015.
89. McBride, J. D.; Leatherbarrow, R. J. *Curr. Med. Chem.* **2001**, *8*, 909.
90. Obrecht, D.; Chevalier, E.; Moehle, K.; Robinson, J. A. *Drug Discovery Today: Technol.* **2012**, *9*, e63.
91. Chevalier, E.; Sellier-Kessler, O.; Jung, F.; De Marco, S.; Lemercier, G.; Zumbrunn, J.; Ludin, C.; Bisang, C.; Moehle, K.; Henze, H.; Gombert, F. O.; Obrecht, D. *Am. J. Respir. Crit. Care Med.* **2009**, *179*, A5652.
92. Lagente, V.; Guénon, I.; Morel, I.; Sellier-Kessler, O.; Chevalier, E. *Am. J. Respir. Crit. Care Med.* **2009**, *179*, A5668.
93. Sellier, O.; Schmitt, M.; Wach, A.; Chevalier, E. *Eur. Respir. J.* **2013**, *42*, 1762.
94. Flotte, T. R. In *Gene Therapy in Lung Disease*; Lenfant, C., Ed.; CRC Press, Taylor & Francis Group: Boca Raton, FL, 2002; pp 407–418. Chapter 16.
95. Flotte, T. R.; Mueller, C. *Hum. Mol. Genet.* **2011**, *20*, R87.
96. Schuster, B. S.; Kim, A. J.; Kays, J. C.; Kanzawa, M. M.; Guggino, W. B.; Boyle, M. P.; Rowe, S. M.; Muzyczka, N.; Suk, J. S.; Hanes, J. *Mol. Ther.* **2014**, *22*, 1484.
97. GOLD Report 2015; http://www.goldcopd.org; http://www.goldcopd.org/guidelines-copd-diagnosis-and-management.html; accessed 20th May, 2015.
98. Chan, S. C.; Leung, V. O.; Ip, M. S.; Shum, D. K. *Am. J. Respir. Cell Mol. Biol.* **2009**, *41*, 620.
99. Chan, S. C.; Shum, D. K.; Ip, M. S. *Am. J. Respir. Crit. Care Med.* **2003**, *168*, 192.
100. Hahn, S.; Gialis, S.; Chowdury, C. S.; Hösli, I.; Hasler, P. *Semin. Immunopathol.* **2013**, *35*, 439.
101. Kambas, K.; Mitroulis, I.; Ritis, K. *Front. Immunol.* **2012**, *3*, 93.
102. Konstan, M. W.; Hilliard, K. A.; Norvell, T. M.; Berger, M. *Am. J. Respir. Crit. Care Med.* **1994**, *150*, 448.
103. Sinden, N. J.; Baker, M. J.; Smith, D. J.; Kreft, J. U.; Dafforn, T. R.; Stockley, R. A. *Am. J. Physiol. Lung Cell. Mol. Physiol.* **2015**, *308*, L179.
104. Greene, C. M.; McElvaney, N. G. *Br. J. Pharmacol.* **2009**, *158*, 1048.
105. Korkmaz, B.; Horwitz, M. S.; Jenne, D. E.; Gauthier, F. *Pharmacol. Rev.* **2010**, *62*, 726.